



## Analysis of terrestrial water storage changes from GRACE and GLDAS

Tajdarul H. Syed,<sup>1</sup> James S. Famiglietti,<sup>1</sup> Matthew Rodell,<sup>2</sup> Jianli Chen,<sup>3</sup> and Clark R. Wilson<sup>4</sup>

Received 28 November 2006; revised 9 August 2007; accepted 8 November 2007; published 22 February 2008.

[1] Since March 2002, the Gravity Recovery and Climate Experiment (GRACE) has provided first estimates of land water storage variations by monitoring the time-variable component of Earth's gravity field. Here we characterize spatial-temporal variations in terrestrial water storage changes (TWSC) from GRACE and compare them to those simulated with the Global Land Data Assimilation System (GLDAS). Additionally, we use GLDAS simulations to infer how TWSC is partitioned into snow, canopy water and soil water components, and to understand how variations in the hydrologic fluxes act to enhance or dissipate the stores. Results quantify the range of GRACE-derived storage changes during the studied period and place them in the context of seasonal variations in global climate and hydrologic extremes including drought and flood, by impacting land memory processes. The role of the largest continental river basins as major locations for freshwater redistribution is highlighted. GRACE-based storage changes are in good agreement with those obtained from GLDAS simulations. Analysis of GLDAS-simulated TWSC illustrates several key characteristics of spatial and temporal land water storage variations. Global averages of TWSC were partitioned nearly equally between soil moisture and snow water equivalent, while zonal averages of TWSC revealed the importance of soil moisture storage at low latitudes and snow storage at high latitudes. Evapotranspiration plays a key role in dissipating globally averaged terrestrial water storage. Latitudinal averages showed how precipitation dominates TWSC variations in the tropics, evapotranspiration is most effective in the midlatitudes, and snowmelt runoff is a key dissipating flux at high latitudes. Results have implications for monitoring water storage response to climate variability and change, and for constraining land model hydrology simulations.

**Citation:** Syed, T. H., J. S. Famiglietti, M. Rodell, J. Chen, and C. R. Wilson (2008), Analysis of terrestrial water storage changes from GRACE and GLDAS, *Water Resour. Res.*, 44, W02433, doi:10.1029/2006WR005779.

### 1. Introduction

[2] Terrestrial water storage (TWS) is defined as all forms of water stored above and underneath the surface of the Earth. TWS is a key component of the terrestrial and global hydrological cycles, exerting important control over the water, energy and biogeochemical fluxes, thereby playing a major role in Earth's climate system [Famiglietti, 2004]. For example, soil water storage affects the partitioning of water and energy fluxes at the land surface, with implications for precipitation recycling, hydrologic extremes including drought and flood and by impacting land memory processes [Shukla and Mintz, 1982; Eltahir and Bras,

1996]. Surface water storage impacts rates of freshwater, sediment and nutrient transport, and plays an important role in greenhouse gas emissions to the atmosphere [Richey *et al.*, 2002]. TWS is a key unknown in the calculation of current rates of global mean sea level rise [Church *et al.*, 2001]; and it impacts Earth rotation variations such as length of day [Chao and O'Connor, 1988]. As an integrated measure of surface and groundwater availability, TWS has significant implications for water resources management.

[3] In spite of its manifold importance, until recently, TWS has not been adequately measured at the continental scale [Lettenmaier and Famiglietti, 2006]. This is primarily due to the lack of a comprehensive global network for routine TWS monitoring. While ground and satellite based techniques can measure some individual components such as soil moisture [Njoku *et al.*, 2003] and surface water [Aldorf and Lettenmaier, 2003], there has been no integrated measurement of TWS.

[4] The dearth of direct observations of large scale TWS estimates was resolved by the launch of Gravity Recovery and Climate Experiment (GRACE) twin satellite mission in March, 2002. Although primarily aimed at accurately mapping time variations in Earth's gravity field at ~30 day

<sup>1</sup>Department of Earth System Science, University of California, Irvine, California, USA.

<sup>2</sup>Hydrological Sciences Branch, NASA Goddard Space Flight Center, Greenbelt, Maryland, USA.

<sup>3</sup>Center for Space Research, University of Texas at Austin, Austin, Texas, USA.

<sup>4</sup>Department of Geological Sciences, University of Texas at Austin, Austin, Texas, USA.

intervals, GRACE has shown remarkable prospects for inferring water mass changes over the globe [Tapley et al., 2004a; Wahr et al., 2004].

[5] Most GRACE hydrology studies to date, including those described above and in section 2 below, have dealt with either comparison of derived terrestrial water storage anomalies (TWSA, i.e., TWS deviations from the mean rather than month to month changes) to models and to limited observations; methods of data processing and error analyses; and to new applications for monitoring TWS components and fluxes. While the capability for GRACE to monitor continental scale anomalies and changes in monthly water storage is now well documented, little if any work has addressed fundamental issues such as the characterization of its space-time variability and its role in terrestrial hydroclimatology, namely how observed TWSC is distributed among the terrestrial subsurface and surface stores, and how the fluxes of precipitation, evapotranspiration and runoff act to enhance or dissipate the storages.

[6] Here we present a detailed analysis of continental scale water storage changes using GRACE and output from a high quality global land hydrological modeling system. Unlike the other studies described here, the emphasis of this work is toward understanding the spatial-temporal variability in the role of different hydrologic fluxes and storages influencing the magnitude and distribution of TWSC over the globe. Note that the lack of global-scale observations of TWSC necessitates a model-based approach to the analyses. In the first part of our work we focus on the characterization of spatial-temporal variability in observed storage changes over land. Total water storage changes are quantified over the different continents and in some of its largest river basins. In the second part we compare estimates of TWSC from GRACE and the Global Land Data Assimilation System (GLDAS; Rodell et al., 2004b). Having demonstrated good agreement between the two, in the third part of the analysis, we discuss the zonal and global patterns of variability in TWSC and how these patterns are controlled by the various hydrologic and climatologic factors, using GLDAS-based states and fluxes.

## 2. Background

[7] GRACE is a joint venture between NASA and the DLR launched in March 2002. The mission objective is to accurately measure the mean and time varying component of Earth's gravity field at monthly timescales for a period of at least 5 years. The mission consists of twin satellites spaced  $\sim 220$  km apart in a near circular polar orbit at an altitude of  $\sim 500$  km. Spatial-temporal variations in Earth's gravity field affect the distance between the two satellites: a continuous and accurate measurement of changes of this distance (inter-satellite range) by the onboard K-Band microwave ranging system [Tapley et al., 2004a], combined with other ancillary data, enables precise maps of Earth's time-variable gravity field to be produced. Over land, time variations of these global gravity fields are primarily due to water mass variations [Wahr et al., 1998; Tapley et al., 2004b]. This has allowed for the first time, observations of variations in TWS at large river basin [Swenson et al., 2003; Chen et al., 2005; Seo et al., 2006; Winsemius et al., 2006] to continental scales [Wahr et al., 2004; Ramillien et al., 2005; Klees et al., 2007]. Extraction of these hydrologic

signals over land by the removal of effects from other time-varying geophysical factors is one of the prime motivations behind the GRACE satellite mission and is an active area of research.

[8] Rodell and Famiglietti [1999, 2001] showed promising results in pre-launch assessment of some of the key aspects of GRACE, such as the potential detectability and accuracy of measuring TWSC, using estimated GRACE errors and modeled and observed water storage data. Since the mission began, several studies have described GRACE's ability to detect water storage changes at varied spatial scales over different parts of the globe [Wahr et al., 2004; Ramillien et al., 2004], to monitor the mass balance of the ice sheets [Velicogna and Wahr, 2006a, 2006b], to quantify fluxes [Rodell et al., 2004a; Syed et al., 2005; Ramillien et al., 2006; Swenson and Wahr, 2006a] and storages [Rodell et al., 2007; Yeh et al., 2006; Frappart et al., 2006a; Schmidt et al., 2006] in land surface hydrology and for the validation and improvement of the terrestrial water balance in global land surface models [Niu and Yang, 2006; Swenson and Milly, 2006]. In addition there are numerous studies addressing different filtering techniques to retrieve water storage change signals and its associated error structures [Seo and Wilson, 2005; Swenson and Wahr, 2002, 2006b; Chen et al., 2005; Ramillien et al., 2005].

[9] Herein we present a study, complementary to earlier studies, but primarily aimed at characterization and understanding of the role of TWSC in terrestrial hydroclimatology. Our overall emphasis is on the analysis of process controls and partitioning of continental water storage changes at varied spatial and temporal scales using state of the art assimilated hydrological model data. This will help us in trying to understand how the terrestrial storage is partitioned at different spatial and temporal scales and how these estimates are affected by the hydrologic fluxes at similar scales.

## 3. Methods

[10] In order to investigate the water storage changes, corrected GRACE Stokes coefficients (Level 2 Gravity Field Product User Handbook, Bettadpur, S., 2003) provided by the Center for Space Research (CSR) at the University of Texas at Austin were expanded to degree and order 60 and smoothed with a 1000 km half-width Gaussian averaging kernel to produce the time varying gravity estimates. The coefficients of the lowest degree zonal harmonics, the degree two and order zero term was not taken into consideration, mainly due to large unquantifiable errors associated with this term. Subsequently these smoothed spherical harmonic coefficients were transformed into  $1 \times 1$  degree gridded data that reflect vertically integrated water mass changes averaged over a few hundred kilometers with an accuracy of  $\sim 1.5$  cm of equivalent water thickness [Wahr et al., 2004]. Since we average gridded land water storage changes over much larger spatial domains for this analysis, the error at these spatial scales is smaller than 0.1 cm/month [Ramillien et al., 2006]. Errors in GRACE data estimated by the above mentioned studies represent a combination of measurement and processing errors, see Wahr et al. [2006] for additional details. The reader is referred to Wahr et al. [1998] and Tapley et al. [2004a] for a more detailed description of the processing of GRACE data. Note that

**Table 1.** GLDAS Variables Used in This Study

Parameters	Spatial Resolution	Temporal Resolution	Time Span	Spatial Extent
Precipitation (Includes both solid and liquid rainfall) (P)	1° × 1°	monthly sum	Jan'02–Dec'04	180°W–180°E 90°N–60°S
Total soil moisture (4 layers from 0–200 cm depth) (TSM)	1° × 1°	monthly average	Jan'02–Dec'04	180°W–180°E 90°N–60°S
Evapotranspiration (E)	1° × 1°	monthly sum	Jan'02–Dec'04	180°W–180°E 90°N–60°S
Runoff (Includes both surface and subsurface flow)(R)	1° × 1°	monthly sum	Jan'02–Dec'04	180°W–180°E 90°N–60°S
Canopy water storage (CWS)	1° × 1°	monthly average	Jan'02–Dec'04	180°W–180°E 90°N–60°S
Snow Water Equivalent (SWE)	1° × 1°	monthly average	Jan'02–Dec'04	180°W–180°E 90°N–60°S

techniques for processing GRACE data continue to evolve and improve [Han *et al.*, 2005; Seo and Wilson, 2005; Swenson and Wahr, 2006a]. The GRACE data set used in this study is CSR RL01 which spans from April 2002 to July 2004 excluding some months in 2002 (May, June and July) and June in 2003. Longer time periods of GRACE data are becoming available and will allow for studies of interannual variations. The impact of the length of the smoothing radius has also been addressed [Chen *et al.*, 2006]. However, for the purposes of this work, the above-described data set sufficiently captures the key features of terrestrial hydroclimatology.

[11] The primary land surface flux and storage component data were obtained from NASA's Global Land Data

respectively, and  $t$  is time. TWS considered here constitutes total column soil moisture (TSM), Snow Water Equivalent (SWE) and Canopy Water Storage (CWS). Neither surface water storage in inland water bodies nor groundwater storage is represented in the model simulations. Both can be important components of TWS in certain regions of the globe [Rodell and Famiglietti, 2001; Frappart *et al.*, 2006b]. Our analysis of storage partitioning is therefore limited to TSM, SWE and CWS and cannot give a complete description of the lateral and vertical distribution of water storage until surface and groundwater components are added to land model used here. Such work is ongoing in our research team. Hence following equation (1), estimates of TWSC from GLDAS that closely approximate GRACE were calculated as follows

$$\left[\frac{\Delta S}{\Delta t}\right]_N = \left[\frac{\{\bar{S}_{soil(15,N)} + \bar{S}_{snow(15,N)} + \bar{S}_{canopy(15,N)}\} - \{\bar{S}_{soil(15-N)} + \bar{S}_{snow(15-N)} + \bar{S}_{canopy(15-N)}\}}{\Delta t}\right] \quad (2)$$

Assimilation System (GLDAS) [Rodell *et al.*, 2004b]. GLDAS parameterizes, forces, and constrains multiple land surface models with ground and satellite observation based data sets, toward the goal of accurate simulation of water and energy cycle states and fluxes. For this study we used 1-degree, 3-hourly output from a 1979-present run of the Noah land surface model [Ek *et al.*, 2003] driven by GLDAS. Because of the model's inability to represent ice sheet flow and mass balance, Antarctic was not simulated and output from Greenland was excluded from the analysis. For this investigation we extracted the relevant hydrological fluxes and storages from January, 2002 to December, 2004, and aggregated them to monthly averages or accumulations as appropriate (Table 1).

[12] GRACE-derived TWSC estimates were obtained by differencing the monthly TWS anomalies, which themselves were obtained by removing the mean gravity field from each of the monthly GRACE solutions. These estimates of TWSC can be interpreted as average changes in TWS from one month to the other.

[13] A comparable replication of GRACE observations from GLDAS land surface output is based on the following equation

$$\left[\frac{\Delta S}{\Delta t}\right]_N = \left[\frac{\bar{S}_{i,N} - \bar{S}_{i,N-1}}{\Delta t}\right] \quad (1)$$

where  $\bar{S}$  represents the average TWS for the indexed day ( $i$ ), the subscripts  $i$  and  $N$  represent day of month and month

[14] The terms on the right hand side are 15th day averages of each calendar month of the year. We assume that an averaged estimate of the 15th day can be considered representative of the  $\sim 30$  day average. The method showed promising results in an earlier study [Syed *et al.*, 2005] and also compared well with other published methods of aggregation of monthly fluxes [Swenson and Wahr, 2006a; Rodell *et al.*, 2004a]. Additionally, TWSC can be computed using a monthly basin-scale terrestrial water balance which can be approximated as follows

$$\left[\frac{\Delta S}{\Delta t}\right]_N = \sum_{N-1}^N P - \sum_{N-1}^N E - \sum_{N-1}^N R \quad (3)$$

where  $P$  is precipitation,  $R$  is runoff and  $E$  is evapotranspiration.

## 4. Results and Discussion

### 4.1. Water Storage Changes from GRACE

[15] In this section we characterize the spatial-temporal variability in the observed water storage change signals from GRACE. The underlying causes of these variations are discussed in more detail in subsequent sections.

[16] Figure 1a shows that the time series of globally averaged TWSC peaks during NH Winter (DJF) with an amplitude of roughly 0.6 centimeters/month. Figure 1b shows the latitudinal distribution of seasonally averaged

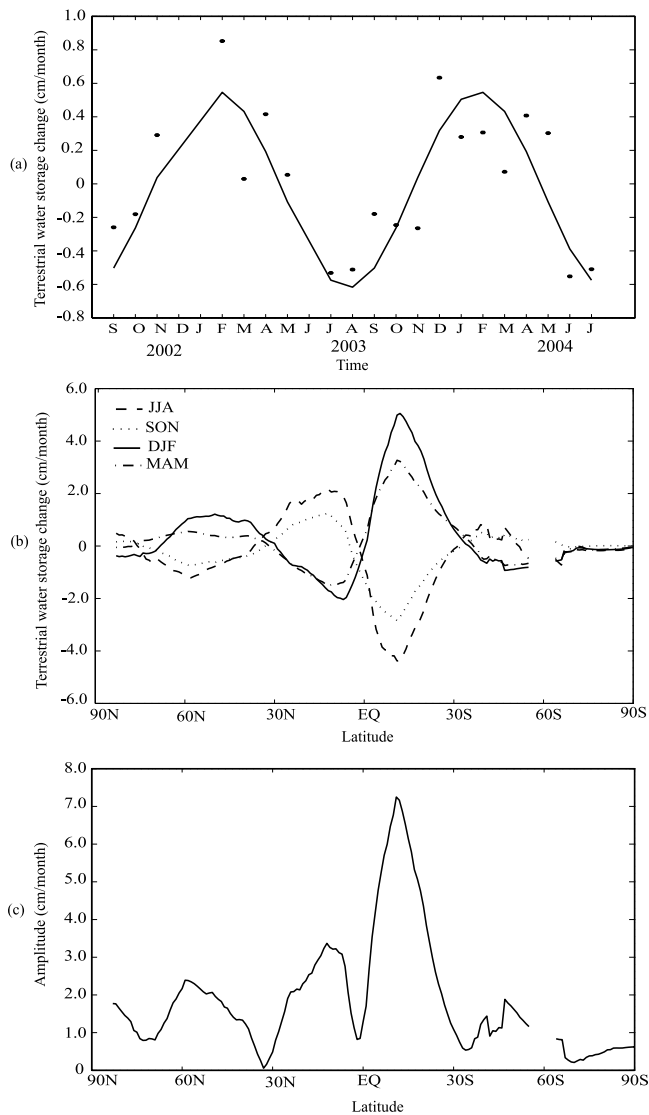


**Figure 1.** (a) Monthly variations of globally averaged GRACE-derived TWSC estimates (black dots) are shown along with the fitted seasonal cycle (black solid line). (b) Zonally averaged TWSC estimates from GRACE for each season, JJA, SON, DJF and MAM. (c) Amplitudes of seasonal cycles fitted to the zonally averaged absolute value of TWSC estimates from GRACE.

TWSC. A clear dominance of the strongest water storage change signals in a Southern Hemisphere (SH)  $0^{\circ}$  to  $30^{\circ}$  S latitudinal band is apparent for all the seasons, with lesser peaks in the NH subtropics and at  $60^{\circ}$ N. In the tropics, Summer (Winter) is dominated by increases (decreases) in TWSC, due to increases (decreases) in precipitation in response to seasonal migration of the ITCZ. In contrast, midlatitudes during JJA (DJF) are dominated by decreases (increases) in TWSC, due to increases (decreases) in evapotranspiration. The polar regions are similar to the tropics, but with slight JJA (DJF) increases (decreases) in TWSC, particularly in the NH. The amplitude of the seasonal cycle in the zonally averaged absolute value of TWSC (Figure 1c) has associated peaks in the corresponding regions.

[17] The TWSC variations in the tropics shown in Figure 1b can be readily explained by the migration and strength of the Inter Tropical Convergence Zone (ITCZ), with maxima associated with enhanced precipitation. The hemispheric differences in the amplitudes of TWSC ( $\pm 4$ – $5$  cm/month in SH;  $\pm 2$  cm/month in NH) are manifestations of greater land precipitation in the SH in comparison to the NH, especially in equatorial South East Asia, South America and Africa [Adler *et al.*, 2003]. Minima correspond to shifts in the subtropical depressions where evapotranspiration increases. In addition to the large fluctuations in the tropics, there is a NH midlatitude zone of much lower yet prominent variability in the range of  $\pm 1$  centimeter/month. Positive storage changes in DJF result from midlatitude polar frontal precipitation and snow storage. Snowmelt and evapotranspiration account for the decreasing (MAM) and negative (JJA, SON) peaks in this zone. Note that the TWSC variations during SON and MAM can be viewed as intermediate stages of the stronger end-members prevalent during JJA and DJF.

[18] The amplitude of seasonal cycle in zonally averaged value of TWSC (Figure 1c) provides perspective on the magnitude of the storage changes, both positive and negative, across the continents. The greatest variation in storage changes occur in the SH Tropics with an amplitude greater than 7 cm/month, followed by the NH Tropics ( $\sim 3.2$  cm/month), the NH midlatitudes ( $\sim 2.4$  cm/month) and the SH midlatitudes (almost 2 cm/month). Figure 1c further highlights where the principal zones for mass exchange between the land and the atmosphere or ocean occur, and that they are consistent with the major features of the atmospheric general circulation and global patterns of precipitation and evaporation [Hartmann, 1994; Peixoto and Oort, 1992]. This also includes the desert regions with zero or low TWSC (near  $30^{\circ}$  N and S).

[19] Figures 1b and 1c have two important implications for terrestrial hydroclimatology. The first is that global scale measurements of TWSC, available for the first time with GRACE, have identified significant regions of dynamic change, and that they are consistent with global patterns of weather and climate. The second, more subtle implication is that the GRACE mission has shown that terrestrial water storage responds in predictable ways to precipitation and evaporation processes, hence providing important “memory” of past atmospheric phenomena.

[20] Table 2 lists the annual means, amplitudes of fitted annual cycles and seasonal means of GRACE-based TWSC, averaged for each continent and the river basins shown in Figure 2. Although insignificant compared to the amplitude of the cycles, annual mean values over Europe, South America and Asia show a net accumulation of water mass with values of 0.32 cm/month, 0.30 cm/month and 0.08 cm/month respectively for the period of the GRACE data used here. On the other hand, even lesser depletion of total water storage is noted in Australia ( $-0.13$  cm/month), North America ( $-0.06$  cm/month) and Africa ( $-0.02$  cm/month). The seasonal means again point to the influence of ITCZ migration on the distribution of land water storage, similar to what we have noted in Figure 1. While tropical basins in the NH gain water (e.g., Yangtze (2.44 cm/month), Ganges/Brahmaputra (4.65 cm/month), Orinoco (2.80 cm/month) and Niger (2.03 cm/month)) during JJA from enhanced precipitation, basins in the SH tropics and those in NH mid-to-high latitudes

**Table 2.** Estimates of Annual Mean, Amplitude of Fitted Annual Cycle and Seasonal Mean for the Continents and the Largest River Basins

Region	Annual Mean, cm/month	Amplitude, cm/month	Seasonal Mean, cm/month			
			DJF	MAM	JJA	SON
<b>North America</b>	-0.06	0.50	0.73	-0.18	-0.34	-0.18
Mississippi	0.30	1.33	1.33	-0.57	-0.06	0.28
Mackenzie	-0.23	1.32	1.87	-0.46	-1.17	-0.89
<b>South America</b>	0.30	4.10	2.44	0.87	-1.45	-1.43
Amazon	0.55	7.60	3.85	1.86	-2.78	-2.69
Parana	0.11	3.41	2.75	-1.03	-0.26	-0.83
Orinoco	0.66	3.27	-2.10	3.23	2.80	-2.73
<b>Asia</b>	0.08	0.60	0.16	0.31	-0.16	-0.10
Yangtze	0.20	2.69	-1.44	0.34	2.44	-1.45
Ganges/Brahmaputra	0.13	5.80	-1.85	-1.30	4.65	-1.02
Amur	0.26	0.46	0.28	0.39	0.05	0.07
Yenisei	-0.11	3.06	1.31	0.62	-2.50	0.42
Ob	0.06	4.21	1.45	1.41	-2.81	0.04
Lena	0.07	1.87	0.66	0.86	-1.93	0.75
<b>Africa</b>	-0.02	0.60	0.05	-0.21	-0.33	0.22
Congo	-0.28	1.95	0.36	-0.72	-2.57	0.96
Nile	-0.12	1.90	-0.32	-1.03	0.99	-0.26
Niger	0.05	4.04	-1.92	-0.18	2.04	0.64
Zambezi	-0.01	5.18	3.20	0.42	-3.40	-0.49
<b>Europe</b>	0.32	3.67	1.81	-0.17	-1.20	0.59
Volga	0.50	4.93	2.27	-0.11	-1.42	0.69
Danube	0.31	4.34	2.87	-0.37	-2.01	0.79
Dniepr	0.58	5.28	3.17	-0.76	-1.16	0.64
Don	0.46	4.84	2.90	-0.32	-1.36	0.56
<b>Australia</b>	-0.14	2.50	1.67	0.13	-1.89	-0.41
Murray	-0.11	1.90	1.01	0.14	-1.34	-0.26

tend to lose water (e.g., Zambezi (-3.40 cm/month), Amazon (-2.80 cm/month), Congo (-2.74 cm/month), Ob (-2.80 cm/month) and Lena (-1.93 cm/month)) due to lack of precipitation and increased evapotranspiration. On the

contrary, basins in the SH tropics tends to gain water during DJF while those in the NH tropics experience a net loss in storage, underscoring the dominant role of climate in defining the spatiotemporal heterogeneity of observed storage change. Furthermore, the amplitude of the annual cycles in South America (4.10 cm/month) stands out from those for the rest of the continents, including the Amazon basin (7.60 cm/month) which has the largest amplitude among the river basins. Amplitudes of variability secondary to those in the Amazon are found in Ganges/Brahmaputra (5.80 cm/month), Dniepr (5.28 cm/month) and Zambezi (5.18 cm/month) river basins.

[21] It is important to note here that, while it is necessary to smooth the Stokes coefficients from GRACE to reduce the noise in derived mass change fields, the process also suppresses the variability of the storage change signal. The length scale used for smoothing further affects the derived storage change estimates. While a large averaging radius can decrease the strength in the storage change signal [Chen et al., 2006], a smaller radius can produce spurious north-south stripes [Swenson and Wahr, 2006b]. Hence our estimates of mean (annual and seasonal) and amplitude of seasonal cycles based on the use of 1000 km half-width Gaussian averaging kernel are conservative characterizations of basin-to-continental storage changes observed by GRACE.

[22] To understand the relative contributions from the large river basins in Figure 2 toward the TWSC for an entire continent, ratios of the sum of absolute value of TWSC in a basin to that of the continent were computed for North America, South America, Africa and Asia. Figure 3 illustrates the relative contributions of some of the largest river basins toward the total storage change in North America, South America, Africa and Asia. Also shown in the figure

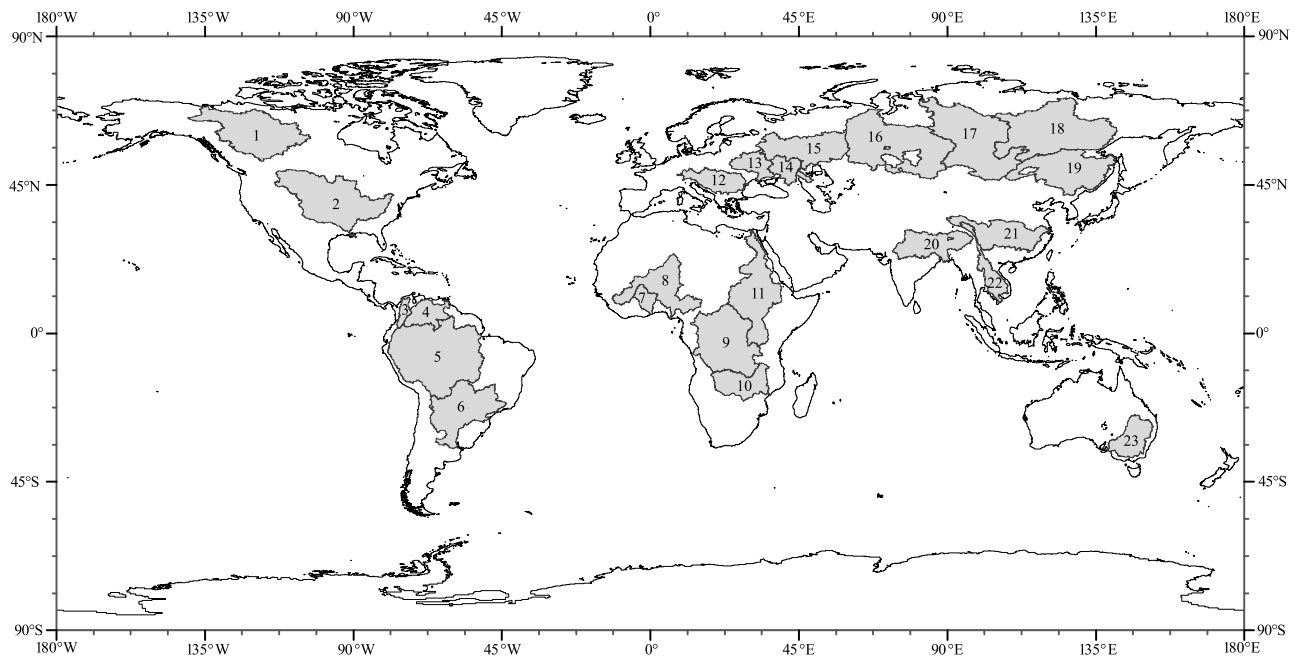


**Figure 2.** River basins referred to in this study: (1) Mackenzie; (2) Mississippi; (3) Magdalena; (4) Orinoco; (5) Amazon; (6) Parana; (7) Volta; (8) Niger; (9) Congo; (10) Zambezi; (11) Nile; (12) Danube; (13) Dniepr; (14) Don; (15) Volga; (16) Ob; (17) Yenisei; (18) Lena; (19) Amur; (20) Ganges/Brahmaputra; (21) Yangtze; (22) Mekong; (23) Murray.

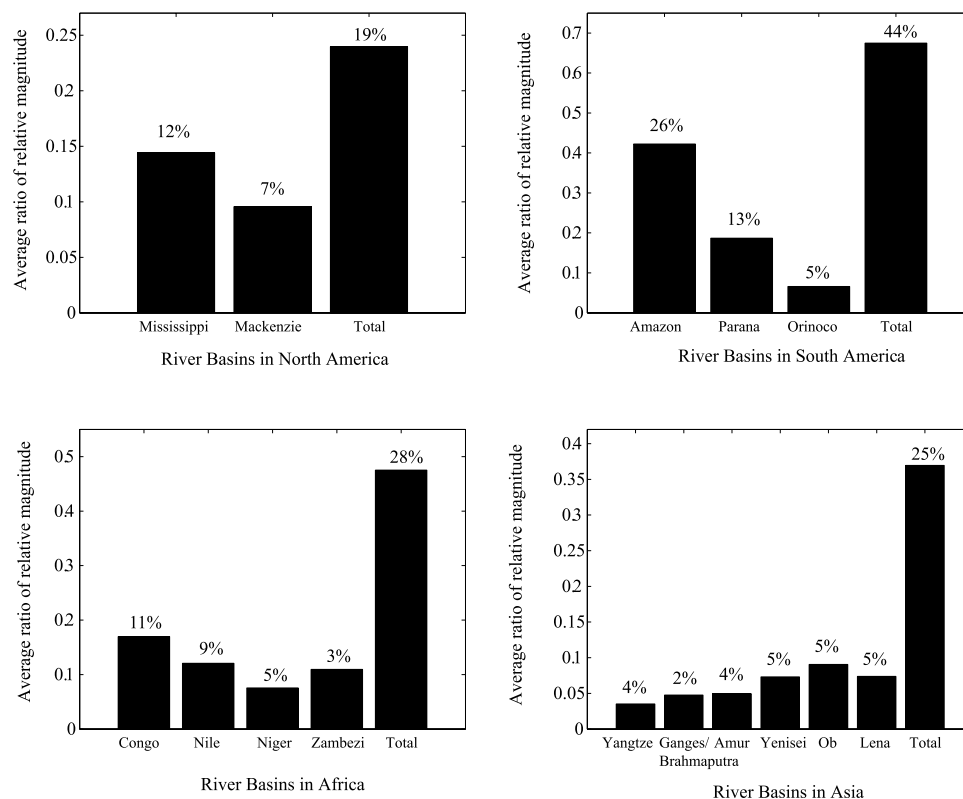


**Figure 3.** Ratio of GRACE-derived TWSC in the listed river basin to that of the entire continent. Total represents the sum of ratios for the river basins considered in each continent. Also shown are (above each bar) the percentage of continental area occupied by each of the river basins.

is the percentage of continental area residing within each of the river basins. The results show that just a few of these river basins can account for a notable portion of the total storage change over the entire continent in which the basins are located. This is particularly noteworthy in continental South America, where the change in the Amazon basin is on average of about 45% of the continental storage change, and the aggregate (Amazon, Parana and Orinoco) contributes about 70% while the contributing area is ~44% of the area of South America. To a lesser degree, similar results are also seen in Africa and Asia, where aggregated storage changes in the basins shown account for 50%, 35% of the continental water storage changes respectively.

#### 4.2. GRACE–GLDAS Comparisons

[23] In this section, we compare seasonal estimates of TWSC from GRACE to those from GLDAS [Rodell *et al.*, 2004b]. For consistency with the GRACE data, TWSC from GLDAS was computed using equations (1)–(2). Although not a perfect reproduction of observations, global model output such as that from GLDAS captures the magnitude and variability of terrestrial hydrology sufficiently enough, so that in the absence of any similar, global observational data sets, it provides a reasonable opportunity for evaluation and understanding of the GRACE hydrology signal [Syed *et al.*, 2004]. For comparison with GRACE, GLDAS-based TWSC estimates were converted into spherical harmonic coefficients, smoothed with a 1000 km half-

width Gaussian averaging kernel and transformed into  $1 \times 1$  degree gridded data.

[24] Global plots of seasonal storage change estimates obtained from GRACE and GLDAS are shown in Figure 4. GLDAS results used here are for the same period as the GRACE measurements. There is very good overall agreement between the two estimates with Root Mean Square Errors (RMSE) ranging between ~1 cm/month in JJA and ~0.7 cm/month in DJF. Some of biggest storage change signals, consistent with Figure 3, are occurring in the Amazon, Ganges/Brahmaputra, Congo river basins and over large regions of Northern Europe and Western North America. While there are some small differences in magnitude of the TWSC estimates, GLDAS performs reasonably in capturing the global spatial patterns of observed storage changes at seasonal timescales.

[25] Time series of TWSC from GRACE and GLDAS for four of the major river basins in continental North and South America are shown in Figure 5. Also included in the plots for Mississippi and Amazon basins are independent estimates of TWSC from a combined land-atmosphere water balance (LAWB) [Syed *et al.*, 2005]. GLDAS estimates agree very well with GRACE, with RMSE values of ~1.5 cm/month in Mississippi and Mackenzie and ~2.5 cm/month in Amazon and Parana river basins. Estimates of storage change from GLDAS and LAWB also track each other fairly well in both the Amazon (RMSE = 4.5 cm/month) and Mississippi (RMSE = 1.6 cm/month) basins except for the periods of September–October in 2002 and late JJA 2003. Discrepan-

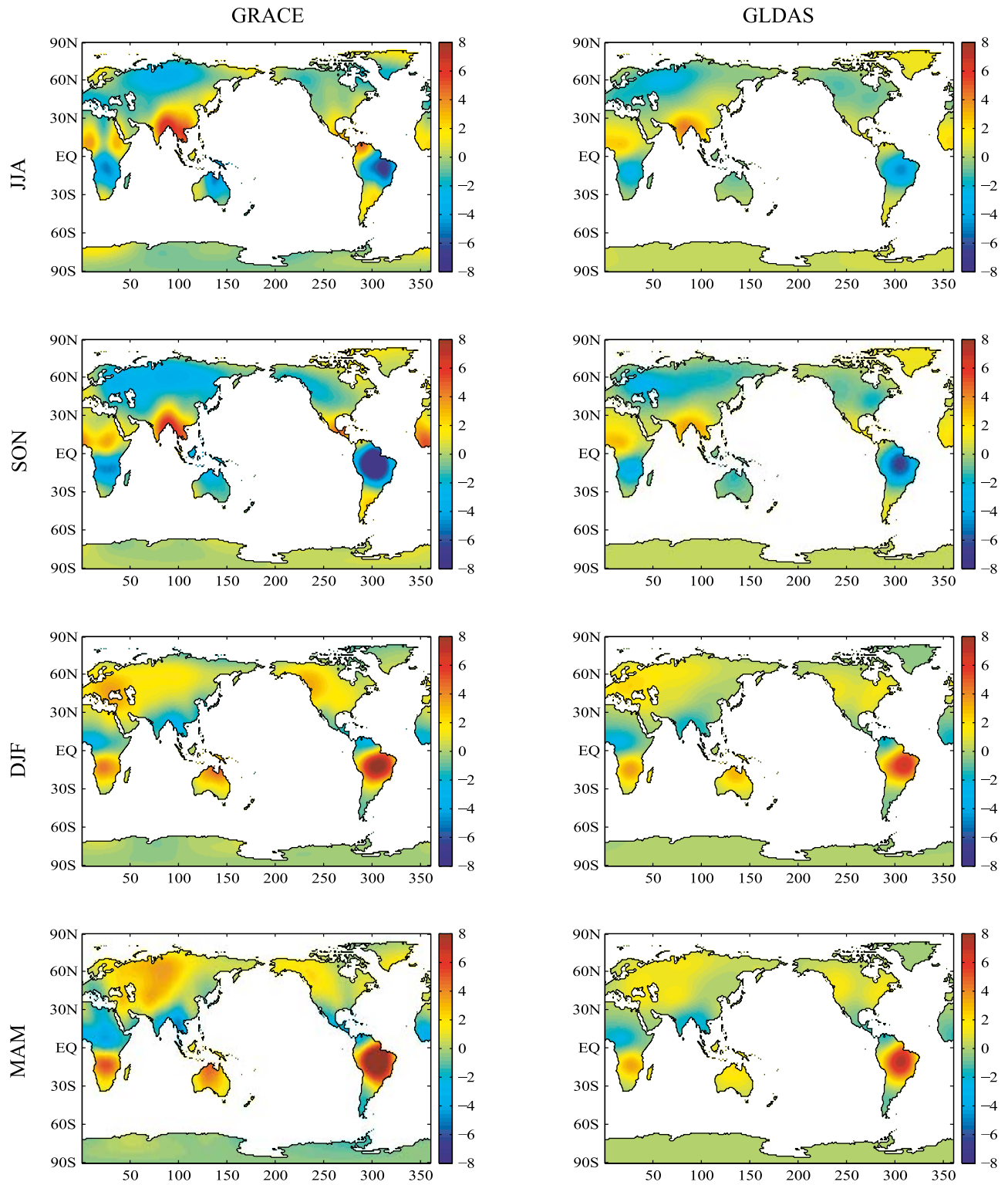


**Figure 4.** Spatial patterns of seasonally averaged TWSC (cm/month) from GRACE and GLDAS. On the basis of the seasonal averages computed for the period of April 2002 till July 2004.

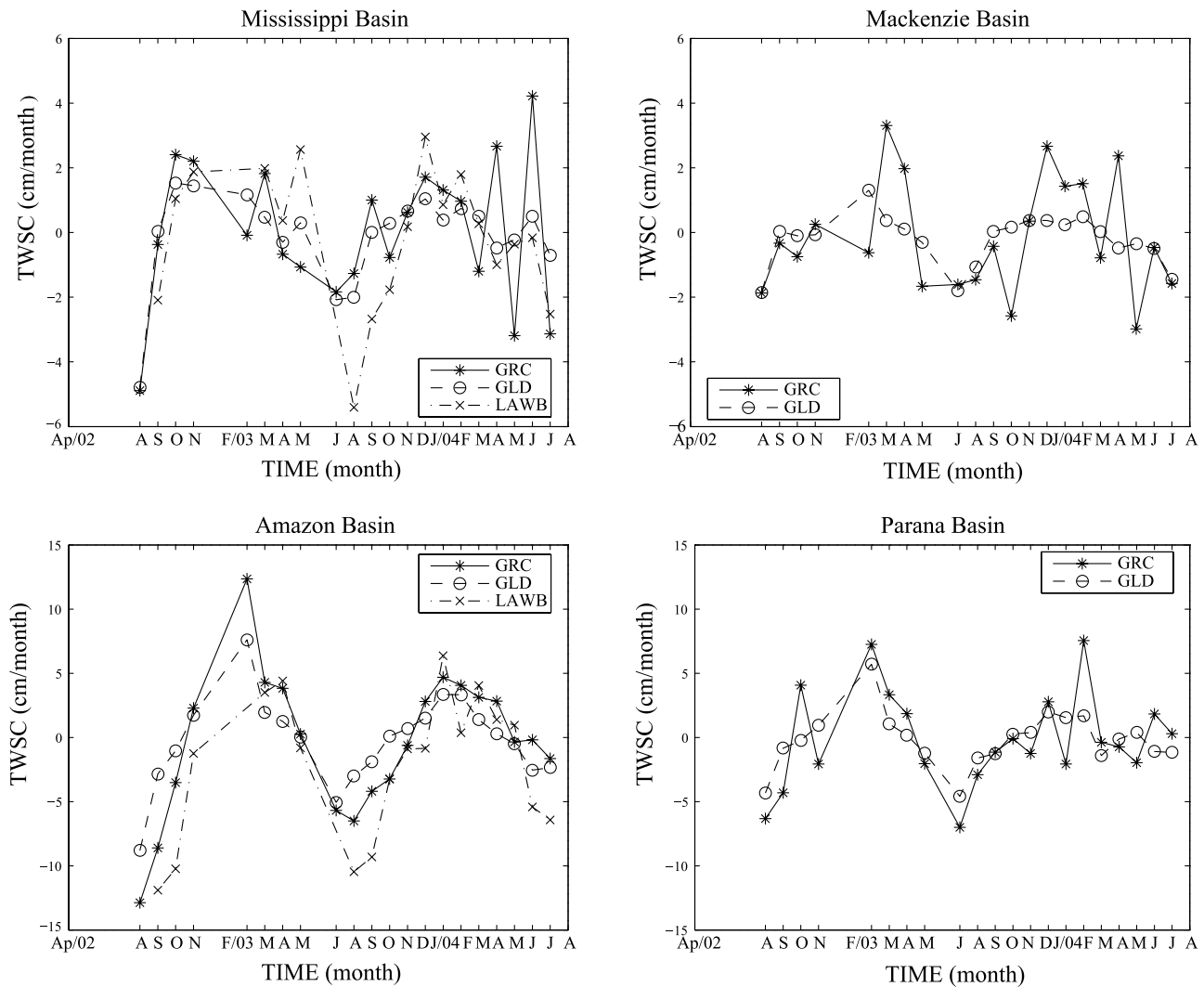


**Figure 5.** TWSC estimates from GRACE (GRC) and GLDAS (GLD) in 4 of the largest river basins in continental North and South America. Also included for Mississippi and Amazon basins are TWSC from a Land-Atmosphere Water Balance (LAWB).

cies between TWSC estimates from GLDAS and LAWB are attributed to errors in the horizontal divergence of water vapor ( $\text{Div}Q$ ) and are discussed in detail by Syed *et al.* [2005]. Furthermore, model estimates of storage change are less variable than GRACE-derived storage changes, primarily due to the absence of contributions from surface and groundwater in the simulations.

[26] Overall, Figures 4 and 5 show good agreement in the spatial-temporal variability of TWSC estimates from GRACE and GLDAS. The differences in magnitude between the two estimates can either be due to model deficiencies, such as inadequate snow or missing surface or groundwater components in the models, or due to uncertainties in the GRACE data (e.g., due to processing, aliasing, instrument error, etc.). One consequence of the GRACE errors is that true water storage change signals may be enhanced or dampened in both regional and global scales [Swenson and Wahr, 2006b; Chen *et al.*, 2006a; Seo and Wilson, 2005]. Nevertheless, we believe that the agreement between GRACE and GLDAS is sufficient, so that GLDAS output fields can be studied to better under-

stand the processes contributing to terrestrial water storage variations.

### 4.3. Analysis of Process Controls in TWSC

#### 4.3.1. Time Series Analysis

[27] Globally averaged TWSC, along with its storage (TSM, SWE and CWS, following equation (2)) and flux (P, E and R) components, obtained from GLDAS, are shown in Figure 6. The annual cycles (solid line) of TWSC and its storage components (Figure 6a) show distinctive seasonal variations with the lowest values during the months of June–July and highs around December of each year. The insignificant role played by CWS in TWSC variations is also clear from the figure so that it is excluded from further discussion.

[28] Changes in TSM and SWE contribute nearly equally toward temporal variability in globally averaged TWSC estimates in terms of both amplitude and phase. SWE estimates, while limited in geographic extent, contribute significantly toward globally averaged TWSC estimates by the virtue of the larger magnitude of snow water storage. On



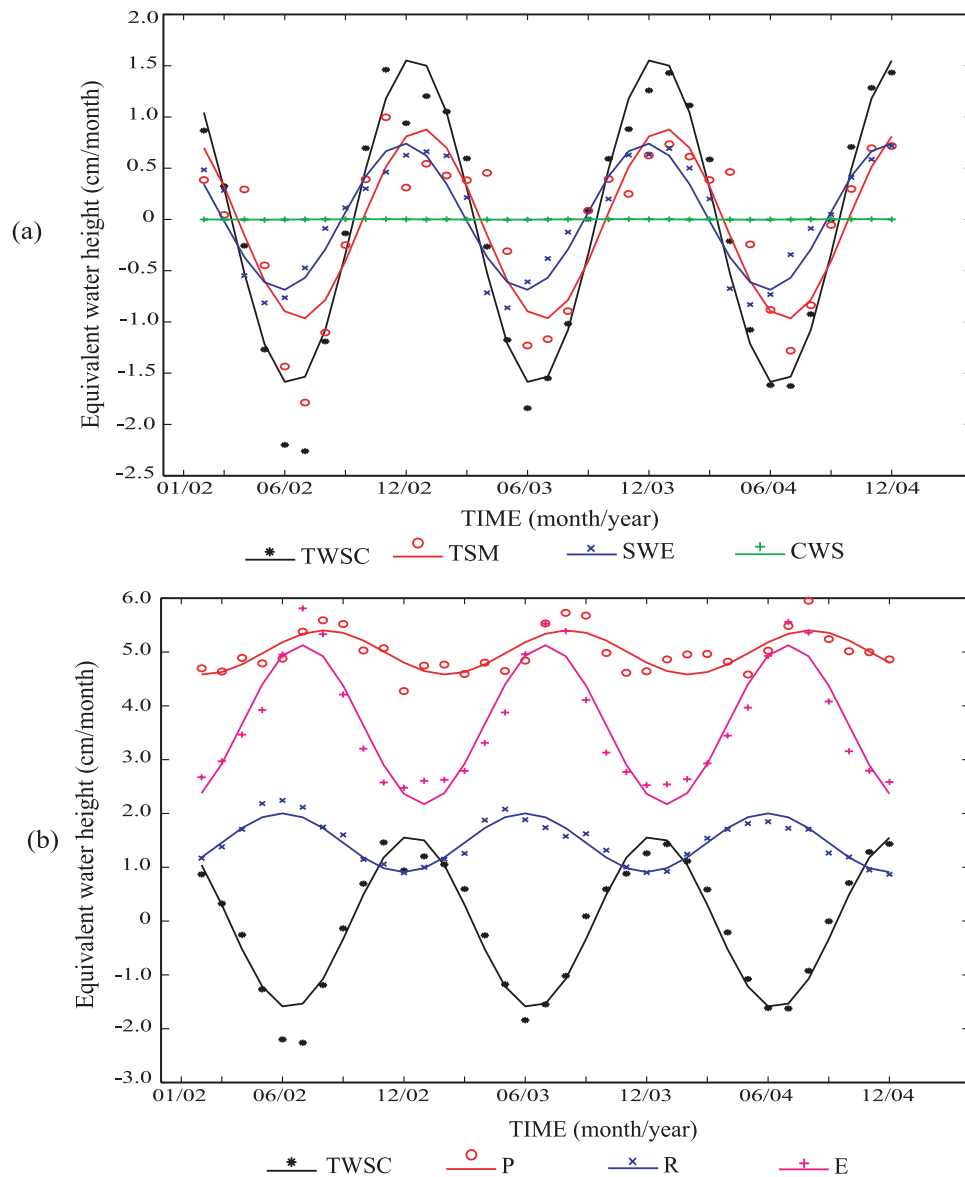


**Figure 6.** (a) Time series of globally averaged TWSC and changes in its storage components: total soil moisture (TSM), snow water equivalent (SWE) and canopy water storage (CWS). (b) Time series of globally averaged TWSC and the hydrologic fluxes, precipitation (P), runoff (R) and evapotranspiration (E). All the variables shown here are based on GLDAS outputs. Shown are the monthly estimates (symbols) and fitted seasonal cycles (solid lines) of each variable in their respective colors.

the other hand TSM estimates have a contrasting feature, i.e., wider spatial extent but smaller magnitudes. Furthermore, peak TSM storage lags that of SWE, indicative of the contribution of snowmelt to soil moisture recharge.

[29] Variations in SWE are driven by NH snow storage, which peaks in DJF. Total soil moisture peaks in DJF and reaches a minimum in JJA. The wetting sequence starts in SON and ends in the following MAM, and is an integrated effect of the monsoons in both the hemispheres and snowmelt episodes. Global soil moisture begins to dry considerably during late-MAM and reaches its lowest in mid-JJA, when evaporation depletes the water stored from the previous season's rain and snowmelt events.

[30] Time series of TWSC flux components (Figure 6b) also show distinct annual periodicity and significantly

greater amplitudes in the variability of E and TWSC in comparison to P and R. The role of E as a major influence on the variability of globally averaged TWSC estimates becomes quite apparent from the similarity in amplitude and cross-varying nature of the estimates (TWSC and E are almost mirror images of each other).

[31] The dominance of NH climatology is reflected in the high and low E values during JJA and DJF, primarily driven by high and low NH insolation respectively. P estimates, although higher in magnitude, have the smallest amplitude among the other fluxes, with highs and lows in late JJA and early MAM respectively. This is also in part due to the greater percentage of land in the Northern Hemisphere. The amplitude of the annual cycle of globally averaged R is also small relative to E, and closely follows the annual cycles of

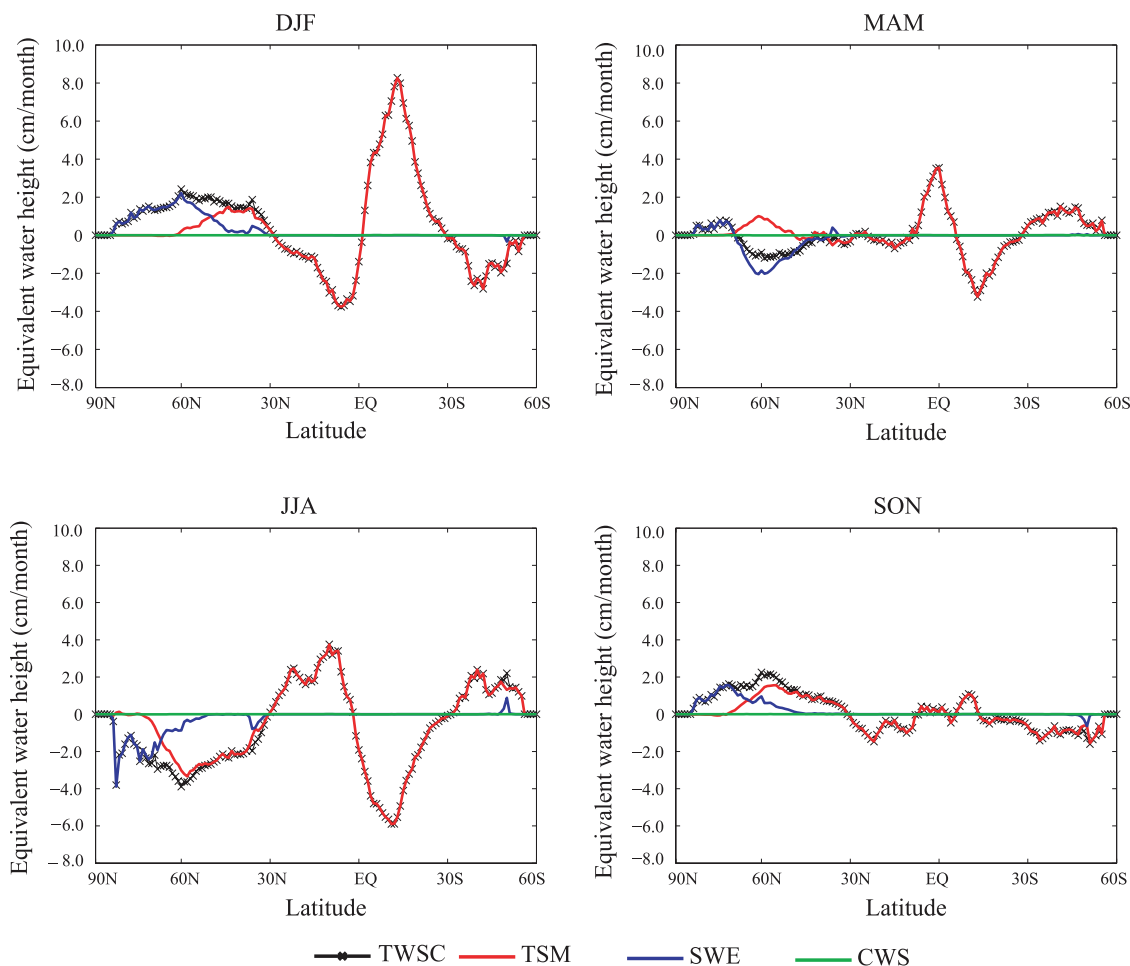


**Figure 7.** Latitudinal profile of zonally averaged TWSC and changes in its storage components (TSM, SWE and CWS) obtained from GLDAS for the four seasons, DJF, MAM, JJA and SON.

P and E. Hence we observe that as P, the sole source of water into the system, increases, so too do E and R, so that globally averaged TWSC and P are actually out-of-phase. The larger amplitude of E dominates annual variations in TWSC.

#### 4.3.2. Spatial Analysis

[32] *Zonal Variability.* In this section we explore how latitudinal variations in GLDAS estimates of TSM and SWE contribute to TWSC, and we characterize how P, E, and R fluxes enhance or dissipate TWSC. Here we focus on seasonal timescales instead of monthly.

[33] Throughout the seasons, changes in TSM contribute the most toward TWSC in the tropics, while SWE is critical in the NH high latitudes (Figure 7). The highest and the lowest values of TWSC and TSM are mainly centered on 15° north and south of the equator. In addition, the plots also reveal seasonal variations in the latitudinal extent of snow dominance in the estimates of storage change. During DJF, SWE begins contributing to TWSC near 40°N latitude, while in JJA the two estimates become closely related nearer to 60°N. As a result we see increased TWSC in the midlatitudes (40°N–60°N) during DJF from snow storage, and a subsequent drop in TWSC values during MAM due to snowpack melting. The role of SWE in high latitudes becomes more evident in MAM, when the values of TWSC

near 60°N drop along with SWE, even with the coinciding increase in total column soil moisture estimates due to soil water recharge by snowmelt.

[34] During SON and MAM, the overall variability of TWSC and its storage components is intermediary in nature when compared to JJA and DJF. In section 4.1 we discussed similar behavior.

[35] The latitudinal variability of TWSC and its component fluxes is shown in Figure 8 for each season. High amplitudes of variability in TWSC estimates along with P, R and E are noted in the ITCZ. As in Figure 1, these high values shift across the equator toward the south during DJF and toward the north during JJA, following the natural variability of the ITCZ.

[36] The principal role of P in controlling the zonal averages of TWSC in the tropics is evident from the zonal profiles of all the seasons. While there is little difference in the estimates of E in the tropics through the seasons, significant seasonal variations are noted in the storage changes of the region, mostly related to P. Storage changes in the midlatitudes are more closely controlled by the E since P decreases away from the tropics.

[37] In addition to the maximum TWSC values found in the tropics, a secondary maxima is located around 60°N and 60°S. Secondary maxima in P in this region result from

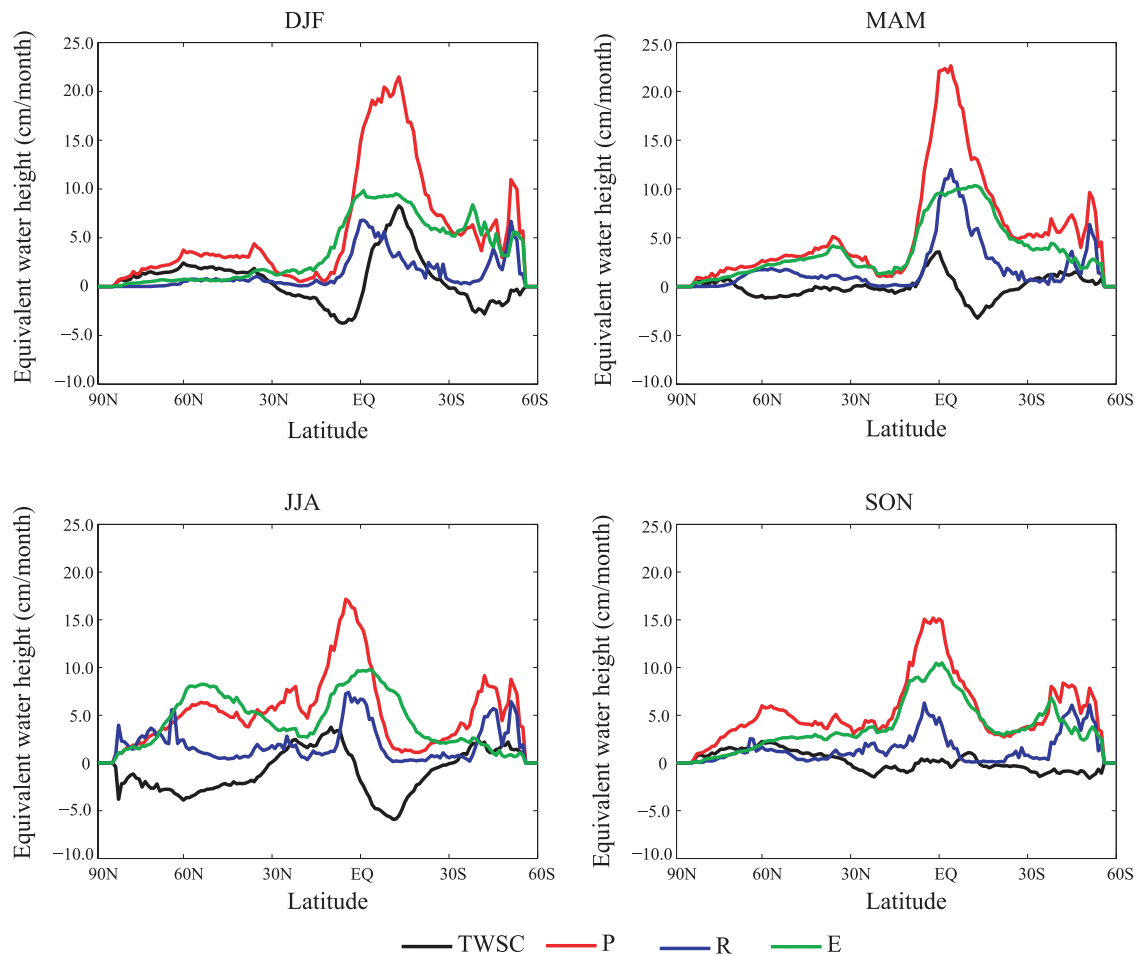


**Figure 8.** Latitudinal profile of zonally averaged TWSC and terrestrial hydrologic fluxes (P, R and E) obtained from GLDAS for the four seasons, DJF, MAM, JJA and SON.

polar frontal convergence. In DJF, low values of E and R contribute to increased TWSC in NH while a significantly increased E in the SH leads to a decrease in TWSC. In MAM and JJA, increases in snowmelt-derived R lead to decreases in TWSC. In fact the MAM and JJA TWSC at the NH mid-to-high latitudes is nearly a mirror image of R due to snow. In summary, we find that P is a dominant control on TWSC variations in the tropics, E plays a critical role in the midlatitudes, while snow accumulation and snowmelt-driven R is significant in at high latitudes.

[38] *Global Variability.* The global distribution of seasonally averaged TWSC and its component fluxes are shown in Figures 9 and 10 for DJF and JJA respectively. Note that different scales are used to portray the spatial heterogeneity over the globe.

[39] Figures 9 and 10 support the ideas outlined above regarding how the various fluxes act to increase or decrease TWSC. However, as discussed in section 4.1, a distinctive feature discernible in all the spatial plots is that the greatest storage changes occur in major river basins over the globe. Some of the key changes in the SH tropics are associated with the Amazon, Parana and Congo river basins and those in the NH with Ganges/Brahmaputra basins in India/Bangladesh along with Mekong in south East Asia and some major African river basins such as the Niger and Volta.

[40] In response to the shifting ITCZ, during DJF, South American river basins north of the equator (Orinoco and Magdalena) are seen to lose water, whereas those located south of the equator (Amazon) gain. Similarly, the river basins above the equator in Africa and South East Asia (Niger, Volta and Ganges/Brahmaputra) tend to lose water during this season and the basins below the equator (Congo and Zambezi) gain water.

#### 4.4. Correlation Analysis

[41] Figure 11 shows the global and latitudinal distribution of the correlation coefficients between monthly GLDAS-based TWSC and the hydrologic fluxes for the entire length of the simulation. P acts as a positive flux in terrestrial water balance; hence areas with positive correlations are interpreted as areas where the values of TWSC are largely impacted by P. On the contrary, evapotranspiration and runoff are variables that deplete water storage; hence negative correlations are indicative of the regions where these processes are most effective in controlling magnitude and variability of the continental water storage changes.

[42] A comparison of the three global correlation plots suggests that positive correlations between precipitation and water storage changes (Figure 11a, first column) have the maximum spatial coverage over the globe followed by the negative correlations between E and R (Figures 11b

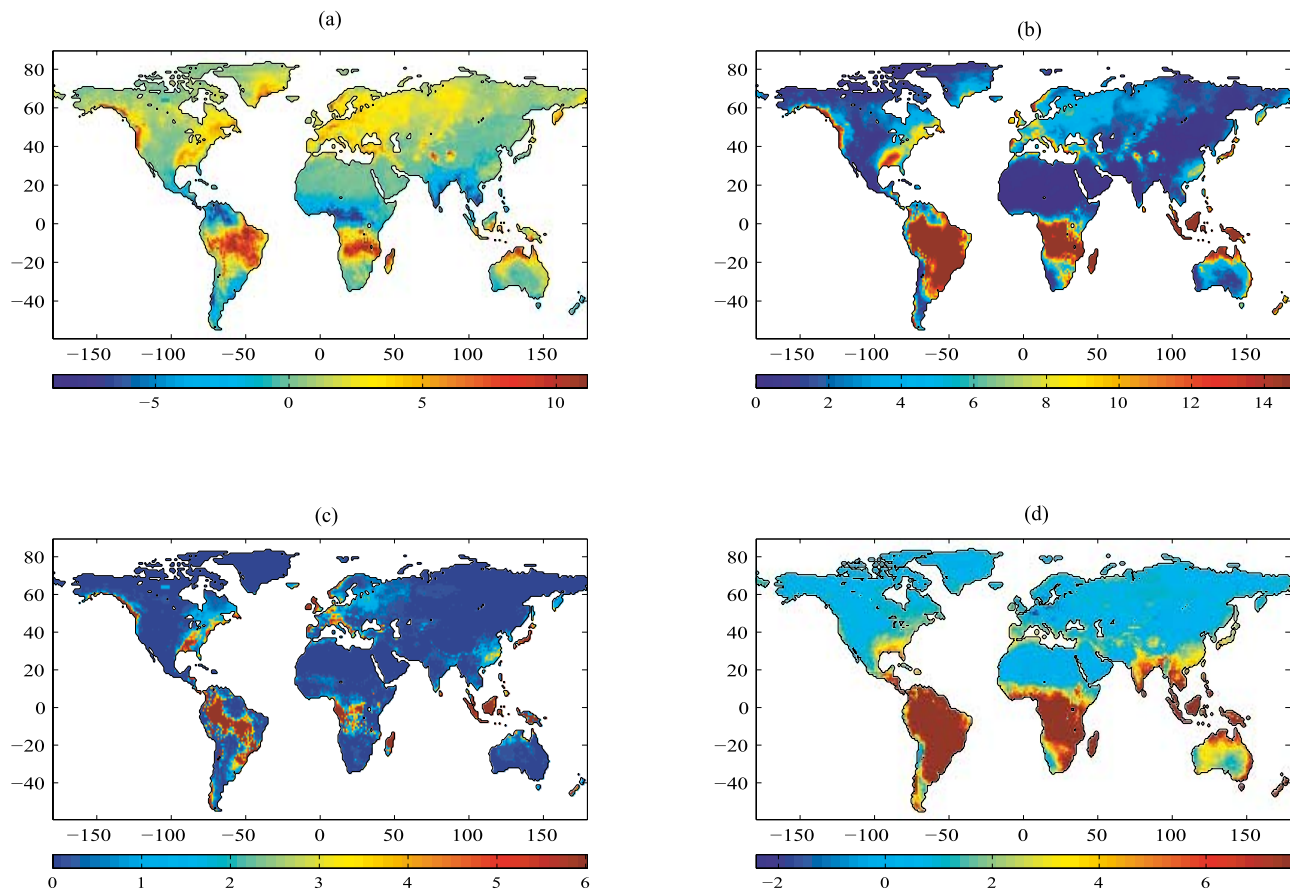


**Figure 9.** DJF average of TWSC and fluxes from GLDAS in cm/month: (a) TWSC; (b) precipitation; (c) runoff; and (d) evapotranspiration.

and 11c, first column). The latitudinal dependence of the controlling processes discussed in the previous section (Figures 9 and 10) is also evident here. The tropics are consistently dominated by the high positive correlations between P and TWSC while the TWSC estimates in the NH midlatitudes are correlated more with E than with P. Figure 11 shows a significant increase in correlation between E and TWSC (Figure 11b, second column) in the region between  $30^{\circ}$ – $70^{\circ}$  N/S and the concomitant decrease in correlation between P and TWSC (Figure 11a, second column). In addition, the dominance of snowmelt-derived runoff in the NH high latitudes is also distinctly discernible from the considerably higher absolute values of correlation between R and TWSC (Figure 11c, second column).

## 5. Summary and Conclusions

[43] In this study we characterize TWSC variations using GRACE and GLDAS. The results discussed here illustrate spatial-temporal variability of water storage changes over land, with implications for a better understanding of terrestrial water balance and its role in the global hydrologic cycle.

[44] Global, zonal and basin-scale estimates of GRACE-based storage changes showed a wide range in variability and magnitude, emphasizing the space-time heterogeneity in TWSC response. Manifestations of hemispheric differences in precipitation were noted in seasonal TWSC. In the SH tropics seasonally averaged TWSC had higher ampli-

tudes ( $\pm 4$ – $5$  cm/month) of latitudinal variability in comparison to those in the NH ( $\pm 2$  cm/month). Zonally averaged TWSC was found to have the greatest amplitude in the SH tropics ( $\sim 7$  cm/month), and the spatial distribution showed major TWSC signals coincident with some of the largest river basins. Comparisons between GLDAS and GRACE-based estimates of TWSC at river basin scales compared well with RMSE of  $\sim 1.5$  cm/month in Mississippi and Mackenzie and  $\sim 2.5$  cm/month in Amazon and Parana.

[45] Analysis of the hydrologic components in the terrestrial water balance from GLDAS revealed the partitioning and process controls of TWSC, both globally and varying with latitude. The Noah land model used in the GLDAS simulations did not include surface and groundwater stores, so that we were unable to quantify their potentially considerable contributions to storage changes in some regions. Global averages of TWSC were found to be partitioned nearly equally between TSM and SWE. Analysis of zonally averaged TWSC showed how storage varies by latitude, with changes in soil moisture accounting for most of the storage change at low and midlatitudes, whereas at high latitudes, TWSC was more closely associated with changes in SWE. Globally averaged estimates of fluxes showed that E plays a key role in dissipating P-driven storage anomalies. Zonal analysis highlighted variations in the role of these fluxes with respect to TWSC. The P flux dominates TWSC variations in the tropics, and E plays a critical role in the midlatitudes. In addition, MAM-

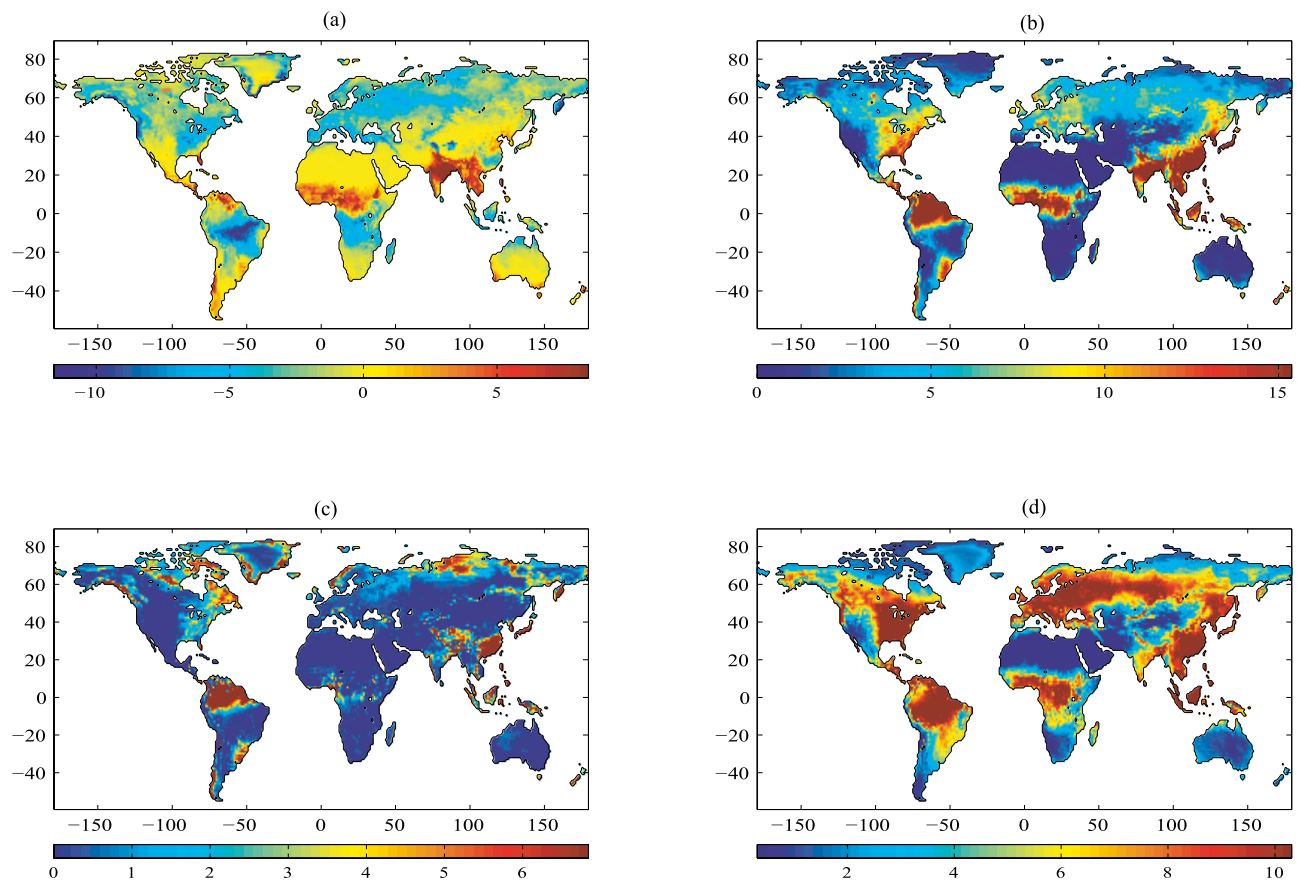


**Figure 10.** JJA average of TWSC and fluxes from GLDAS in cm/month: (a) TWSC; (b) precipitation; (c) runoff; and (d) evapotranspiration.

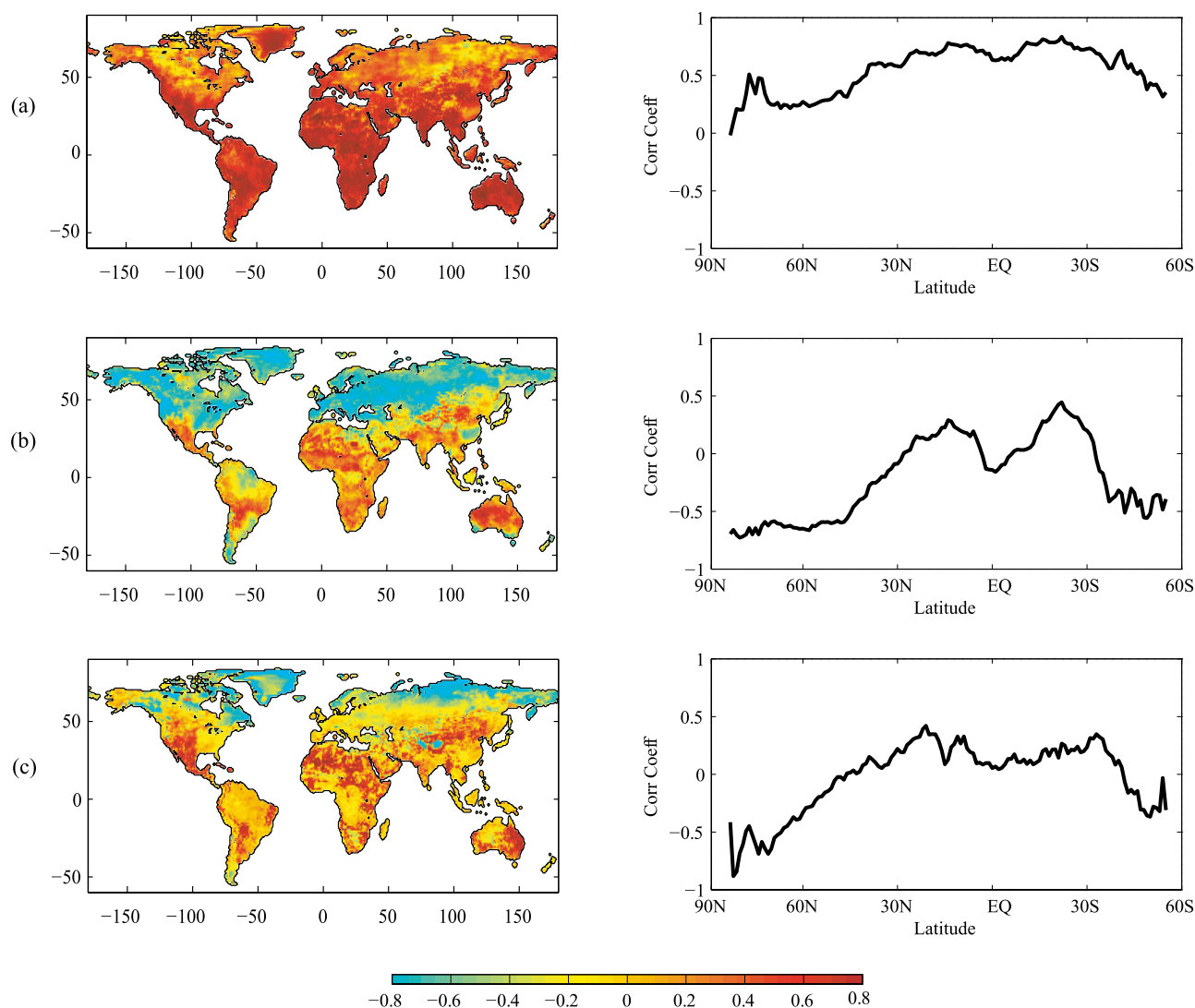


**Figure 11.** Spatial and latitudinal distribution of the correlation coefficients between GLDAS-based TWSC and (a) P; (b) E; and (c) R.

snowmelt-runoff played a particularly important role in space-time variability of TWSC in the NH high latitudes. The results were further reconfirmed by the correlation analysis, which showed P as the leading flux over major portions of the globe, followed by E in the midlatitudes and R in the NH high latitudes.

[46] Comparison of GRACE-based TWSC with GLDAS model simulations also underscores the potential for validating and improving global land surface models [Swenson and Milly, 2006; Niu and Yang, 2006; Lettenmaier and Famiglietti, 2006] using GRACE data. Some of the noted differences between GRACE-based TWSC and GLDAS can in part be attributed to the missing surface and groundwater components, or snow parameterization deficiencies. For example, Niu and Yang [2006] and Niu et al. [2007] showed better agreement with GRACE storage anomalies after including a groundwater component in their land surface parameterization. Future work will be directed toward analysis and comparison of GRACE observations with multiple hydrological models with and without explicit representation of surface and groundwater components in order to fully characterize their role in TWS variations.

Results also suggest that with longer time series, GRACE will contribute to improved understanding of how terrestrial water storage responds to climate change and variability.

[47] **Acknowledgments.** This research was sponsored by NASA grants NNG04GE99G, NNG04GF22G and a NASA Earth System Science Fellowship to the first author, with additional support from the NASA Terrestrial Hydrology and Solid Earth and Natural Hazards Programs.

## References

- Adler, R. F., et al. (2003), The version-2 global precipitation climatology project (GPCP) monthly precipitation analysis (1979–present), *J. Hydro-meteorol.*, *4*(6), 1147–1167.
- Alsford, D. E., and D. P. Lettenmaier (2003), Tracking fresh water from space, *Science*, *301*, 1491–1494.
- Chao, B. F., and W. P. O'Connor (1988), Global surface-water-induced seasonal-variations in the Earth's rotation and gravitational-field, *Geophys. J. Int.*, *94*, 263–270.
- Chen, J. L., C. R. Wilson, J. S. Famiglietti, and M. Rodell (2005), Spatial sensitivity of the Gravity Recovery and Climate Experiment (GRACE) time-variable gravity observations, *J. Geophys. Res.*, *110*, B08408, doi:10.1029/2004JB003536.
- Chen, J. L., C. R. Wilson, J. S. Famiglietti, and M. Rodell (2006), Attenuation effect on seasonal basin-scale water storage changes from GRACE time-variable gravity, *J. Geod.*, doi:10.1007/s00190-006-0104-2.

- Church, J. A., et al (2001), Changes in sea level in *Climate Change 2001: The Scientific Basis*, J. T. Houghton et al. Eds. Cambridge University Press, pp 639–694.
- Ek, M. B., K. E. Mitchell, Y. Lin, E. Rogers, P. Grunmann, V. Koren, G. Gayno, and J. D. Tarpley (2003), Implementation of Noah land surface model advances in the National Centers for Environmental Prediction operational mesoscale Eta model, *J. Geophys. Res.*, 108(D22), 8851, doi:10.1029/2002JD003296.
- Eltahir, E. A. B., and R. L. Bras (1996), Precipitation recycling, *Rev. Geophys.*, 34(3), 367–378.
- Famiglietti, J. S. (2004), Remote sensing of terrestrial water storage, soil moisture and surface waters, in *The state of the planet: Frontiers and challenges in geophysics*, *Geophys. Monogr. Sr.*, vol. 150, edited by R. S. J. Sparks and C. J. Hawkesworth, pp. 197–207, AGU, Washington D. C.
- Frappart, F., G. Ramillien, S. Biancamaria, N. M. Mognard, and A. Cazenave (2006a), Evolution of high-latitude snow mass from the GRACE gravity mission (2002–2004), *Geophys. Res. Lett.*, 33, L02501, doi:10.1029/2005GL024778.
- Frappart, F., K. Do Minh, J. L’Hermitte, A. Cazenave, G. Ramillien, T. Le Toan, and N. Mognard-Campbell (2006b), Water volume change in the lower Mekong basin from satellite altimetry and imagery data, *Geophys. J. Int.*, 167(2), 570–584.
- Han, S.-C., C. K. Shum, C. Jekeli, and D. Alsdorf (2005), Improved estimation of terrestrial water storage changes from GRACE, *Geophys. Res. Lett.*, 32, L07302, doi:10.1029/2005GL022382.
- Hartmann, D. L. (1994), *Global Physical Climatology*, International Geophysics Series, v 56, pp-411, Academic Press, San Diego.
- Klees, R., E. A. Zapreeva, R. C. Winsemius, and H. H. G. Savenije (2007), The bias in GRACE estimates of continental water storage variations, *Hydrol. Earth Syst. Sci.*, 11, 1227–1241.
- Lettenmaier, D. P., and J. S. Famiglietti (2006), Water from on high, *Nature*, 444, 562–563.
- Niu, G.-Y., and Z.-L. Yang (2006), Assessing a land surface model’s improvements with GRACE estimates, *Geophys. Res. Lett.*, 33, L07401, doi:10.1029/2005GL025555.
- Niu, G.-Y., Z.-L. Yang, R. E. Dickinson, L. E. Gulden, and H. Su (2007), Development of a simple groundwater model for use in climate models and evaluation with Gravity Recovery and Climate Experiment data, *J. Geophys. Res.*, 112, D07103, doi:10.1029/2006JD007522.
- Njoku, E. G., T. J. Jackson, V. Lakshmi, T. K. Chan, and S. V. Nghiem (2003), Soil moisture retrieval from AMSR-E, *IEEE Trans. Geosci. Remote Sens.*, 41, 215–229.
- Peixoto, J. P., and A. H. Oort (1992), *Physics of Climate*, pp-564, AIP Press, New York.
- Ramillien, G., A. Cazenave, and O. Brunau (2004), Global time variations of hydrological signals from GRACE satellite gravimetry, *Geophys. J. Int.*, 158, 813–826, doi:10.1111/j.1365-246X.2004.02328.x.
- Ramillien, G., F. Frappart, A. Cazenave, and A. Guntner (2005), Time variations of land water storage from an inversion of 2 years of GRACE geoids, *Earth Planet. Sci. Lett.*, 235, 283–301.
- Ramillien, G., F. Frappart, A. Güntner, T. Ngo-Duc, A. Cazenave, and K. Laval (2006), Time variations of the regional evapotranspiration rate from Gravity Recovery and Climate Experiment (GRACE) satellite gravimetry, *Water Resour. Res.*, 42, W10403, doi:10.1029/2005WR004331.
- Richey, J. E., J. M. Melack, A. K. Aufdenkampe, V. M. Ballester, and L. L. Hess (2002), Outgassing from Amazonian rivers and wetlands as a large tropical source of atmospheric CO<sub>2</sub>, *Nature*, 416, 617–620.
- Rodell, M., and J. S. Famiglietti (1999), Detectability of variations in continental water storage from satellite observations of the time dependent gravity field, *Water Resour. Res.*, 35(9), 2705–2724, doi:10.1029/1999WR900141.
- Rodell, M., and J. S. Famiglietti (2001), An analysis of terrestrial water storage variations in Illinois with implications for the Gravity Recovery and Climate Experiment (GRACE), *Water Resour. Res.*, 37(5), 1327–1340, doi:10.1029/2000WR900306.
- Rodell, M., J. S. Famiglietti, J. Chen, S. I. Seneviratne, P. Viterbo, S. Holl, and C. R. Wilson (2004a), Basin scale estimates of evapotranspiration using GRACE and other observations, *Geophys. Res. Lett.*, 31, L20504, doi:10.1029/2004GL020873.
- Rodell, M., et al. (2004b), The global land data assimilation system, *Bull. Am. Meteorol. Soc.*, 85, 381–394.
- Rodell, M., J. Chen, H. Kato, J. Famiglietti, J. Nigro, and C. Wilson (2007), Estimating ground water storage changes in the Mississippi River basin (USA) using GRACE, *Hydrogeol. J.*, 15(1), 159–166, doi:10.1007/s10040-006-0103-7.
- Schmidt, R., P. Schwintzer, F. Flechtner, C. Reigber, A. Güntner, P. Döll, G. Ramillien, A. Cazenave, S. Petrovic, H. Jochmann, and J. Wünsch (2006), GRACE observations of changes in continental water storage, *Global Planet. Change*, 50, 112–126, doi:10.1016/j.gloplacha.2004.11.018.
- Seo, K.-W., and C. R. Wilson (2005), Simulated estimation of hydrological loads from GRACE, *J. Geod.*, 78, 442–456, doi:10.1007/s00190-004-0410-5.
- Seo, K.-W., C. R. Wilson, J. S. Famiglietti, J. L. Chen, and M. Rodell (2006), Terrestrial water mass load changes from Gravity Recovery and Climate Experiment (GRACE), *Water Resour. Res.*, 42, W05417, doi:10.1029/2005WR004255.
- Shukla, J. Y., and Mintz (1982), Influence of land-surface evapo-transpiration on the Earths climate, *Science*, 215, 1498–1501.
- Swenson, S. C., and P. C. D. Milly (2006), Climate model biases in seasonality of continental water storage revealed by satellite gravimetry, *Water Resour. Res.*, 42, W03201, doi:10.1029/2005WR004628.
- Swenson, S., and J. Wahr (2002), Methods for inferring regional surface-mass anomalies from Gravity Recovery and Climate Experiment (GRACE) measurements of time-variable gravity, *J. Geophys. Res.*, 107(B9), 2193, doi:10.1029/2001JB000576.
- Swenson, S. C., and J. Wahr (2006a), Estimating large-scale precipitation minus evapotranspiration from GRACE satellite gravity measurements, *J. Hydrometeorol.*, 7(2), 252–270, doi:10.1175/JHM478.1.
- Swenson, S., and J. Wahr (2006b), Post-processing removal of correlated errors in GRACE data, *Geophys. Res. Lett.*, 33, L08402, doi:10.1029/2005GL025285.
- Swenson, S., J. Wahr, and P. C. D. Milly (2003), Estimated accuracies of regional water storage variations inferred from the Gravity Recovery and Climate Experiment (GRACE), *Water Resour. Res.*, 39(8), 1223, doi:10.1029/2002WR001808.
- Syed, T. H., V. Lakshmi, E. Paleologos, D. Lohmann, K. Mitchell, and J. S. Famiglietti (2004), Analysis of process controls in land surface hydrological cycle over the continental United States, *J. Geophys. Res.*, 109, D22105, doi:10.1029/2004JD004640.
- Syed, T. H., J. S. Famiglietti, J. Chen, M. Rodell, S. I. Seneviratne, P. Viterbo, and C. R. Wilson (2005), Total basin discharge for the Amazon and Mississippi river basins from GRACE and a land-atmosphere water balance, *Geophys. Res. Lett.*, 32, L24404, doi:10.1029/2005GL024851.
- Tapley, B. D., S. Bettadpur, M. Watkins, and C. Reigber (2004a), The gravity recovery and climate experiment: Mission overview and early results, *Geophys. Res. Lett.*, 31, L09607, doi:10.1029/2004GL019920.
- Tapley, B. D., S. Bettadpur, J. C. Ries, P. F. Thompson, and M. M. Watkins (2004b), GRACE measurements of mass variability in the Earth system, *Science*, 305, 503–505.
- Velicogna, I., and J. Wahr (2006a), Measurements of time-variable gravity show mass loss in Antarctica, *Science*, 311(5768), 1754–1756.
- Velicogna, I., and J. Wahr (2006b), Acceleration of Greenland ice mass loss in Spring 2004, *Nature*, 443(7109), 329–331.
- Wahr, J., M. Molenaar, and F. Bryan (1998), Time variability of the Earth’s gravity field: Hydrological and oceanic effects and their possible detection using GRACE, *J. Geophys. Res.*, 103(B12), 30,205–30,230, doi:10.1029/98JB02844.
- Wahr, J., S. Swenson, V. Zlotnicki, and I. Velicogna (2004), Time-variable gravity from GRACE: First results, *Geophys. Res. Lett.*, 31, L11501, doi:10.1029/2004GL019779.
- Wahr, J., S. Swenson, and I. Velicogna (2006), Accuracy of GRACE mass estimates, *Geophys. Res. Lett.*, 33, L06401, doi:10.1029/2005GL025305.
- Winsemius, H. C., H. H. G. Savenije, N. C. vandeGiesen, B. J. J. M. vandenHurk, E. A. Zapreeva, and R. Klees (2006), Assessment of Gravity Recovery and Climate Experiment (GRACE) temporal signature over upper Zambezi, *Water Resour. Res.*, 42, W12201, doi:10.1029/2006WR005192.
- Yeh, P. J.-F., S. C. Swenson, J. S. Famiglietti, and M. Rodell (2006), Remote sensing of groundwater storage changes in Illinois using the Gravity Recovery and Climate Experiment (GRACE), *Water Resour. Res.*, 42, W12203, doi:10.1029/2006WR005374.

J. Chen, Center for Space Research, University of Texas at Austin, Austin, TX, USA.

J. S. Famiglietti and T. H. Syed, Department of Earth System Science, University of California, Irvine, CA, USA. (jfamigli@uci.edu)

M. Rodell, Hydrological Sciences Branch, NASA Goddard Space Flight Center, Greenbelt, MD, USA.

C. R. Wilson, Department of Geological Sciences, University of Texas at Austin, Austin, TX, USA.